Effects of *Lecanicillium lecanii* strain JMC-01 on the physiology, biochemistry, and mortality of *Bemisia tabaci* Q-biotype nymphs

Ting Xie [1], **Ling Jiang** [1], **Jianshe Li** [1], **Bo Hong** [1], **Xinpu Wang** [1], **Yanxia Jia** [Corresp. 1]

[1] School of Agriculture, Ningxia University, Yinchuan, Ningxia, China

Corresponding Author: Yanxia Jia
Email address: helenjia_2006@nxu.edu.cn

Background. *Lecanicillium lecanii* is an entomopathogenic fungi, which was isolated from insects suffering from disease. Now, it is an effective bio-control resource that can control agricultural pests such as whitefly and aphids. There are many studies on the control of various agricultural pests by *L. lecanii*, but no report on its control of *Bemisia tabaci* biotype-Q exists. In this work we studied the susceptibility of *B. tabaci* Q-biotype (from Ningxia, China) to *L. lecanii* JMC-01 in terms of nymph mortality and the changes in detoxifying protective enzymes activities. **Methods.** *Bemisia tabaci* nymphs were exposed to *L. lecanii* JMC-01 conidia by immersion with the host culture. Mortality was assessed daily for all nymph stages. The detoxifying and protective enzyme activity changes, weight changes, and fat, and water contents of the nymphs were determined spectrophotometrically. **Results.** All instars of *B. tabaci* died after being infested with 1×10^8 conidia/mL. The 2nd-instar nymphs were the most susceptible, followed by the 3rd-instar nymphs. The corrected cumulative mortality of the 2nd- and 3rd-instar nymphs was 82.22% and 75.55%, respectively. The levels of detoxifying and protective enzymes initially increased and then decreased. The highest activities of carboxylesterase (CarE), acetylcholinesterase (AchE), peroxidase (POD), and catalase (CAT) occurred on the 3rd day, reaching 10.5 U/mg prot, 0.32 U/mg prot, 20 U/mg prot, and 6.3 U/mg prot, respectively. These levels were 2.2-fold, 4.3-fold, 2.4-fold, and 1.4-fold the control levels, respectively. The highest activities of glutathione-S transferase (GSTs) and superoxide dismutase (SOD) on the 2nd day were, respectively, 64 U/mg prot and 43.5 U/mg prot. These levels were, respectively, 2.7-fold and 1.1-fold that of the control level. The water and fat content in the infected *B. tabaci* nymphs decreased and differed significantly from the control levels. The weight increased continuously in the first 24 h, decreasing thereafter. At 72 h, the infestation level was about 0.78-fold that of the control level. **Conclusions.** The studied *L.*

lecanii JMC-01 strain is pathogenic to the *B. tabaci* Q-biotype. This strain interferes with the normal functioning of detoxifying and protective enzymes, and is also involved in the disruption of normal physiological metabolism in *B. tabaci*.

Effects of *Lecanicillium lecanii* strain JMC-01 on the physiology, biochemistry, and mortality of *Bemisia tabaci* Q-biotype nymphs

Ting Xie, Ling Jiang, Jianshe Li, Bo Hong, Xinpu Wang, Yanxia Jia*

School of Agriculture, Ningxia University, Yinchuan, China

*Corresponding Author:

Yanxia Jia

College of Agriculture, Ningxia University, No.489, He-Lan-Shan West Road, Xixia, Yinchuan, 750021, People's Republic of China.

Email address: helenjia_2006@nxu.edu.cn.

Abstract

Background. *Lecanicillium lecanii* is an entomopathogenic fungi, which was isolated from insects suffering from disease. Now, it is an effective bio-control resource that can control agricultural pests such as whitefly and aphids. There are many studies on the control of various agricultural pests by *L. lecanii*, but no report on its control of *Bemisia tabaci* biotype-Q exists. In this work we studied the susceptibility of *B. tabaci* Q-biotype (from Ningxia, China) to *L. lecanii* JMC-01 in terms of nymph mortality and the changes in detoxifying protective enzymes activities.

Methods. *Bemisia tabaci* nymphs were exposed to *L. lecanii* JMC-01 conidia by immersion with the host culture. Mortality was assessed daily for all nymph stages. The detoxifying and protective enzyme activity changes, weight changes, and fat, and water contents of the nymphs were determined spectrophotometrically.

Results. All instars of *B. tabaci* died after being infested with 1×10^8 conidia/mL. The 2nd-instar nymphs were the most susceptible, followed by the 3rd-instar nymphs. The corrected cumulative mortality of the 2nd- and 3rd-instar nymphs was 82.22% and 75.55%, respectively. The levels of detoxifying and protective enzymes initially increased and then decreased. The highest activities of carboxylesterase (CarE), acetylcholinesterase (AchE), peroxidase (POD), and catalase (CAT) occurred on the 3rd day, reaching 10.5 U/mg prot, 0.32 U/mg prot, 20 U/mg prot, and 6.3 U/mg prot, respectively. These levels were 2.2-fold, 4.3-fold, 2.4-fold, and 1.4-fold the control levels, respectively. The highest activities of glutathione-S transferase (GSTs) and superoxide dismutase (SOD) on the 2nd day were, respectively, 64 U/mg prot and 43.5 U/mg prot. These levels were, respectively, 2.7-fold and 1.1-fold that of the control level. The water and fat content in the infected *B. tabaci* nymphs decreased and differed significantly from the control levels. The weight increased continuously in the first 24 h, decreasing thereafter. At 72 h, the infestation level was about 0.78-fold that of the control level.

Conclusions. The studied *L. lecanii* JMC-01 strain is pathogenic to the *B. tabaci* Q-biotype. This strain interferes with the normal functioning of detoxifying and protective enzymes, and is also involved in the disruption of normal physiological metabolism in *B. tabaci*.

Introduction

The whitefly or tobacco whitefly *Bemisia tabaci* (Gennadius) (Hemiptera: Aleyrodidae) is a cosmopolitan insect pest with more than 900 documented host plant species. This species is considered to belong to a cryptic species complex with more than 40 morphotypes distributed across the biotypes, with the B- and Q-biotypes being the most important (Tang et al., 2018). The whitefly is of economic importance due to its direct (by sapping plant fluids and vectoring plant pathogens) and indirect (phytosanitary and quarantine measures) damage to crops (Barro, 2011; Xu et al., 2014). Its control mainly relies on chemical pesticide application, which has resulted in the development of insecticide resistance. In addition to the emergence of resistant strains, farms and other stakeholders are challenged by safety concerns. Pesticide application causes environmental pollution, alters the abundance of natural enemies, increases pest resistance and promotes secondary pest population resurgence (Liu et al., 2009). Environmentally-friendly pest management methods, such as biological control using natural enemies and entomopathogen microorganisms (bacteria, fungi and viruses) are being established worldwide in response to this.

Entomopathogenic fungi were the first microorganisms identified as insect pathogens, whereas entomopathogenic bacteria were the first to be commercialized (Lacey et al., 2001) . *Lecanicillium lecanii* [=*Verticillium lecanii* (Zimmerman)Viegas] belongs to Deuteromycotina, Hyphomycetes, Moniliales, Moniliaceae, that is widely use entomopathogenic fungi in bio-control up to now. And the entomopathogenic fungal species described and commercialized, *Lecanicillium lecanii* (Zare and Gams, 2001) deserves further consideration as a broad range commercial biopesticide, due to its wide range of hosts and wide geographical distribution (Xie et al., 2015). Indeed, this species can infect the diamondback moth *Plutella xylostella* (L.) (Lepidoptera: Plutellidae) (Keppanan et al., 2018), aphids (Hemiptera: Aphididae) (Askary et al., 1999), the citrus mealybug *Planococcus citri Risso* (Hemiptera: Pseudococcidae) (Ghaffari et al., 2017), and the soybean cyst nematode *Heterodera glycines* Ichinohe (Tylenchida: Heteroceridae) (Shinya et al., 2008), and has also been documented to infect *B. tabaci* (Zhu and Kim, 2011). In insects, the spores of entomopathogenic fungi germinate, and the fungal hyphae penetrate the epidermis and invade the tissues and organs until reaching the haemocoel (Duan et al., 2017). When the hyphae come into contact with the hemolymph, the defense system of the insects, which includes detoxifying and protective enzymes, is induced (Liu et al., 2013).

Physiological and biochemical approaches have been used to describe the chronological events leading to fungal infestation success in an insect host. Reactive oxygen species (ROS) are forms of atmospheric oxygen (Tian et al., 2016b) produced in the mitochondria that are equilibrated by cellular antioxidative mechanisms (Esmail et al., 2018). In many instances, microbial pathogens are associated with an increase in ROS, which induces an oxidative stress response in the host (Foyer and Noctor, 2013). The antioxidative mechanism of the cells includes

antioxidant enzymes, such as catalase (CAT), superoxide dismutase (SOD) and peroxidase (POD), which degrade H_2O_2 to reduce oxidative damage (Felton and Summers, 1995). In addition to this antioxidative mechanism, insects also harbor detoxifying enzymes, such as carboxylesterase (CarE), glutathione-S transferase (GST), and acetylcholinesterase (AchE), which are able to metabolize exogenous toxicants (Xu et al., 2006), and have been the target of insecticide synergist research (Wang et al., 2016). The effects of these insect detoxifying enzymes in response to the fungal entomopathogen *L. lecanii* in the spiraling whitefly *Aleurodicus dispersus* Russell (Hemiptera: Aleyrodidae) have recently been demonstrated (Liu et al., 2013). These changes in defensive enzymes are deserving further attention, due to its practical considerations.

Due to the lack of studies and the economic importance of *B. tabaci*, the objective of this study was to determine the pathogenic effect of *L. lecanii* strain JMC-01 at the nymphal stages of *B. tabaci* by evaluating the disruption of immune mechanisms.

Materials & Methods

Entomopathogen strain and insect collection

Lecanicillium lecanii strain: the *L. lecanii* strain JMC-01 was isolated from *B. tabaci* infected nymphs from a greenhouse in Yinchuan, Ningxia (N 38°33′, E 106°08′), China in May 2017. The JMC-01 strain was deposited at the China Center for Type Culture Collection (CCTCC) with the accession number M 2018303. The strain status was determined based on ITS sequence divergence to the reference strain (Jiang, 2018). The JMC-01 strain reference ITS nucleotide sequence was deposited in GenBank with the identification number MH312006.

Insect: the whitefly *B. tabaci* Q-biotype was collected from a tomato greenhouse in Yinchuan, Ningxia (N 38°33′, E 106°08′) in July 2018. Biotype assignment was performed as previously described (Gao, 2018). The tomato cultivar Bijiao was planted in a greenhouse in Yinchuan, Ningxia (N 38°33′, E 106°08′) and cultivated using drip irrigation technology. Tomato was used as the host plant for two generations, following which the synchronized nymphs were collected for experimentation.

Preparation of the *L. lecanii* JMC-01 conidial suspension

The *L. lecanii* JMC-01 strain was inoculated on potato dextrose agar (PDA) plates, at 28°C with a 12:12 (L:D, light:dark) photoperiod for 7 d (MJ-250 Mould Incubator, Jiangsu Zhengji Instruments Co. Ltd., Jiangsu, China). Spore suspensions were prepared by recovering the conidia from the PDA plates with a 0.05% Tween-80 solution. The solution was filtered with sterile cheesecloth to eliminate the hyphae, following which the concentration was adjusted to 1.0×10^8 conidia/mL with sterile water using a hemocytometer (Qiujing, Shanghai, China).

Bemisia tabaci nymph mortality induced by *L. lecanii* JMC-01

Tomato leaves with 1st-, 2nd-, 3rd-or 4th-instar nymphs (only one leaf was selected for each instar nymph) were immersed in *L. lecanii* JMC-01 solution at 1.0×10^8 conidia/mL for, 30s or in a control solution of 0.05% Tween-80. After immersion, each leaf was sealed in a standard Petri dish, with its petiole wrapped in a moistened cotton ball. The plates were incubated in an artificial climate chamber (RQX-250, Shanghai Yuejin Medical Devices Co., Ltd., Shanghai, China) at 28±2°C, 70±10% RH, and 12:12 (L:D) photoperiod. There were three replicates per treatment. Deaths were recorded daily, and the cumulative corrected mortality was calculated as follows:

$$\text{Accumulative corrected mortality (\%)} = \frac{\text{Infection mortality} - \text{Control mortality}}{1 - \text{Control mortality}} \times 100\%$$

Susceptibility of 3rd-instar *B. tabaci* nymphs to different JMC-01 concentrations

The *L. lecanii* JMC-01 suspensions were prepared as described above at different conidial concentrations: 1×10^8, 1×10^7, 1×10^6, 1×10^5, and 1×10^4 conidia/mL.

Three tomato leaves with 3rd-instar *B. tabaci* nymphs were immersed for, 30 s at each JMC-01 test concentration, and the leaves were incubated as described above. Deaths were recorded on a daily basis, and were used to determine the cumulative corrected mortality for each conidial concentration.

Protective and detoxifying enzyme activity determination

Tomato leaves with 3rd-instar *B. tabaci* nymphs were infected with *L. lecanii* JMC-01 at 1×10^8 conidia/mL, using the immersion procedure described above. Treated and control (0.05% Tween-80) leaves were immersed in *L. lecanii* JMC-01 solution at 1.0×10^8 conidia/mL for 30 s. After immersion, each leaf was sealed in a standard Petri dish, with its petiole wrapped in a moistened cotton ball. The plates were incubated in an artificial climate chamber (RQX-250, Shanghai Yuejin Medical Devices Co., Ltd., Shanghai, China) at 28±2°C, 70±10% RH, and 12:12 (L:D) photoperiod.

Sample processing: the animal tissue, was weighted and nine-times the volume of normal saline by weight was added [weight(g):volume (ml) = 1:9], the samples were then ground with liquid nitrogen to make a 10% tissue homogenate, which was then centrifuged at 2500 rpm for 10 min (Sigma D-37520, Sigma-Aldrich, Germany). The supernatant was then diluted to 1% tissue homogenate with normal saline for experimentation.

Protein content determination:

The 563 μg/mL standard solution, working fluid, stop application solution and normal saline were purchased from the Jian Cheng Bioengineering Institute (Nanjing, China).

After combining the solutions, they were placed at room temperature for 5 min, and measured colorimetrically at 562 nm (L5S UV spectrophotometer, Shanghai Yidian Analytical Instrument Co., Ltd., Shanghai, China) (Table 1). Double-distilled water served as the blank control.

The protein concentration was determined as follows:

$$\text{Protein (μgprot/mL)} = \frac{\text{Measure OD} - \text{Blank OD}}{\text{Standard OD} - \text{Blank OD}} \times \text{Standard solution (563 μg/mL)} \times \text{Sample dilution before determination}$$

SOD activity determination:

Reagent one application solution, reagent two solution, reagent three solution, reagent four application solution, chromogen solution and normal saline were purchased from the Jian Cheng Bioengineering Institute, Nanjing.

After combining the solutions, they were placed at room temperature for 10 min, and measured colorimetrically at 550 nm (Table 2). Double-distilled water served as the blank

control.

SOD activity was determined as follows:

$$\text{SOD (U/mgprot)} = \frac{\text{Control OD} - \text{Measure OD}}{\text{Control OD}} \div 50\% \times \frac{\text{Total volume of reaction solution}}{\text{Sample size (mL)}} \div \text{Protein concentration of the sample to be tested (mgprot/mL)}$$

POD activity determination:

Reagent one solution, reagent two application solution, reagent three application solution, reagent four solution and normal saline were purchased from the Jian Cheng Bioengineering Institute, Nanjing.

The solutions were combined and centrifuged at 3500 rpm for 10 min (Sigma D-37520, Sigma-Aldrich, Germany), following which the supernatant was measured colorimetrically at 420 nm (Table 3). Double-distilled water served as the blank control.

POD activity was determined as follows:

$$\text{POD (U/mgprot)} = \frac{\text{Measure OD} - \text{Blank OD}}{12 \times 1} \times \frac{\text{Total volume of reaction solution}}{\text{Sample size (mL)}} \div \text{Reaction time (30 min)} \div \text{Protein concentration of the sample to be tested (mgprot/mL)} \times 1000$$

CAT activity determination:

Reagent one solution, reagent two solution, reagent three solution, reagent four solution and normal saline were purchased from the Jian Cheng Bioengineering Institute, Nanjing.

After combining the solutions, they were measured colorimetrically at 405 nm (Table 4). Double-distilled water served as the blank control.

CAT activity was determined as follows:

$$\text{CAT (U/mgprot)} = (\text{Control OD-Measure OD}) \times 271 \times \frac{1}{60 \times 0.05} \div \text{Protein concentration of the sample to be tested (mgprot/mL)}$$

192

193 **CarE activity determination:**

194 The working fluid and normal saline were purchased from the Jian Cheng Bioengineering
195 Institute, Nanjing.

196 Sample processing: the sample processing was as described in the protein content
197 determination step above, except that the tissue homogenate was centrifuged at 12000 rpm for 4
198 min.

199 The steps were as follows:

200 ① The spectrophotometer was preheated for at least 30 min and the wavelength was adjusted to
201 450 nm. The machine was blanked with double-distilled water.

202 ② The working fluid was preheated at 37 °C for at least 30 min.

203 ③ Blank tube: 5 μL of distilled water was added to a blank glass cuvette, to which 1000 μL of
204 preheated working solution was sequentially added to a 1 mL glass cuvette. The solution was
205 rapidly mixed, and light absorption A_1 and A_2 was measured at 450 nm10 s and 190 s,
206 $\Delta A_{Blank\ tube}=A_2-A_1$.

207 ④ Measuring tube: 5 ul of supernatant was sequentially added to a 1 ml glass cuvette, 1000 ul
208 of preheated working solution, and rapidly mixed, and light absorption of A_3 and A_4 were
209 measured at 450 nm, $\Delta A_{Measuring\ tube}=A_4-A_3$.

210 CarE (U/mgprot) = $(\Delta A_{Measuring\ tube} - \Delta A_{Blank\ tube}) \times V \div (Cpr \times V_{Sample}) \div T$

211 V: total volume of the reaction solution, 1.005 mL;

212 Cpr: protein concentration of the sample to be tested (mgprot/mL);

213 V_{Sample}: adding of supernatant volume to the reaction system (mL), 0.005 mL；

214 T: catalytic reaction time (min), 3 min。

215

AchE activity determination:

1 μmol/ml standard application solution, substrate buffer, chromogen application solution, inhibitor solution, transparent solution and normal saline were purchased from the Jian Cheng Bioengineering Institute, Nanjing.

After combining the solutions, they were placed at room temperature for 15 min and measured colorimetrically at 412 nm (Table 5). Double-distilled water served as the blank control.

AchE activity was determined as follows:

$$\text{AchE (U/mgprot)} = \frac{\text{Measure OD} - \text{Control OD}}{\text{Standard OD} - \text{Blank OD}} \times \text{standard concentration (1 μmol/mL)} \div$$

Protein concentration of the sample to be tested (mgprot/mL)

GST activity determination:

Matrix fluid, reagent two application solution, anhydrous alcohol, GSH strandard application solution, 20 μmol/ml GSH strandard solution, reagent three application solution, reagent four application solution and normal saline were purchased from the Jian Cheng Bioengineering Institute, Nanjing.

Enzymatic reaction:

The solutions were combined and centrifuged at 3500 rpm for 10 min (Sigma D-37520, Sigma-Aldrich, Germany) (Table 6). The supernatant was then used in the chromogen reaction.

Chromogen reaction:

The solutions were combined and placed at room temperature for 15 min, following which they were measured colorimetrically at 412 nm (Table 7). Double-distilled water served as the blank control.

GST activity was determined as follows:

$$\text{GST (U/mgprot)} = \frac{\text{Control OD} - \text{Messure OD}}{\text{Strandard OD} - \text{Blank OD}} \times \text{strandard concentration (20 μmol/mL)} \times$$

Reaction system dilution factor (6 times) ÷Reaction time (10 min) ÷ [Sample volume (0.1 mL) × Protein concentration of the sample to be tested (mgprot/mL)]

242

243 **Determination of weight, and water and fat content of the *B. tabaci* nymphs after**
244 **infestation with *L. lecanii* JMC-01**

245 Tomato leaves with 3rd-instar *B. tabaci* nymphs exposed to 1.0×10^8 conidia/mL or the control
246 treatment (0.05% Tween-80). The treated and control leaves were placed in similar Petri dishes.
247 Following this method was used, the same Petri dish method as above was then used.

248 The treatment and control group were selected one hundred 3rd-instar nymphs for
249 experimentation after 0 h, 12 h, 24 h, 36 h, 48 h, 60 h and 72 h, respectively. First determining
250 the total fresh weight of 100 nymphs prior to infection (Mettler Toledo LE204E/02 electronic
251 balance), the nymphs were dried by placing each batch at 60°C for 48 h in an electrothermal
252 blowing dry box (Shanghai Yiheng Technology Co., Ltd., Shanghai, China), and weighed in a
253 similar method as for the determination of dry weight (dry mass, DM).

254 Water content (WC) was determined using the formula WC =(FW-DM)/FW×100%, where
255 DW is the dry mass determined as explained above, and FW is the fresh weight determined as
256 above.

257 Lipid extraction was performed with the dried nymphs. The dried nymphs were grinded under
258 liquid nitrogen in a centrifuge tube. One mL of chloroform isoamyl alcohol (24:1) and 0.5 mL of
259 methanol (99.99%) was added to each tube, mixed, and then centrifuged at 4500 rpm for 10 min.
260 The supernatant was discarded. The precipitate was extracted again with 1 mL of chloroform
261 isoamyl alcohol (24:1) and 0.5 mL of methanol (99.99%) by centrifugation at 4500 rpm for 10
262 min. The final remaining precipitate was dried in an oven at 60°C for 48 h to determine the
263 constant dry mass (LDM).

264 Fat content (FC) was determined using the formula FC = (DM-LDM) / DM ×100%, where
265 DM is the dry mass determined as explained above, and LDM is the constant dry mass
266 determined after lipid extraction.

267 There were three replicates per treatment and time point, and 100 nymphs per replicate.

268

269 **Data analysis**

270 Excel 2010 (Microsoft Corporation, Albuquerque, NM, USA) was used to process all the data.
271 All results are expressed as the mean ± standard deviation (SD). Statistical analysis of the data

was performed using one-way analysis of variance (ANOVA) with SPSS version 21.0 (SPSS, IBM Corp., Armonk, NY, USA). Multiple comparisons of the means were performed using Duncan's (D) tests at a significance level of P = 0.05. All figures were produced using Origin 8.0.

Results

Morphological characteristics of the *B. tabaci* nymphs

Figure 1 shows the morphological characteristics of *B. tabaci* under *L. lecanii* JMC-01 infection as observed under a microscope (Leica Microsystems Wetzlar GmbH). The surface is covered with hyphae.

Mortality of the *B. tabaci* nymphs

Figure 2 indicates the cumulative mortality induced by *L. lecanii* JMC-01 to each *B. tabaci* immature stage. The cumulative corrected mortality of the nymph instars was as follows (from high to low): 2^{nd} instar >3^{rd} instar >1^{st} instar >4^{th} instar >egg. The 2^{nd}- and 3^{rd}-instar nymphs were most affected, with corrected cumulative mortality percentages of 82.22% and 75.55%, respectively.

The initial dose of *L. lecanii* JMC-01 affects the 3^{rd}-instar *B. tabaci* nymphs

As indicated in Fig. 3, increasing doses of *L. lecanii* JMC-01 (from $1x10^4$ to $1x10^8$ conidia/mL) also increased the corrected cumulative mortality of the 3^{rd}-instar nymphs, reaching a maximum of 75.55% at 1×10^8 conidia/mL after 6 d.

Protective and detoxifying enzyme activity determination

The highest activity of SOD (43 U/mg prot) was detected on the 2^{nd} day, reaching 1.1-fold that of the control (Fig. 4). The highest activities of POD and CAT were 20 U/mg prot and 6.3 U/mg prot on the 3^{rd} day, respectively, and reached 2.4-fold and 1.4-fold that of the control level (Fig. 5, Fig. 6). Following this, the activities of protective enzymes decreased. The lowest activities of

SOD, POD, and CAT were 30 U/mg prot, 8.5 U/mg prot, and 1.3 U/mg prot on the 5th day, respectively (Fig. 4, Fig. 5, Fig. 6).

The highest activities of CarE and AchE were 10.5 U/mg prot and 0.32 U/mg prot. These levels were observed on the 3rd day and were 2.2-fold and 4.3-fold that of the control level, respectively (Fig. 7, Fig. 8). The highest GST activity was 64 U/mg prot on the 2nd day and was 2.7-fold that of the control level (Fig. 9). After the 3rd day, the activities of detoxifying enzymes decreased, and the lowest activities of CarE, AchE, and GST respectively reached 3.5 U/mg prot, 15 U/mg prot, and 0.05 U/mg prot on the 5th day (Fig. 7, Fig. 8, Fig. 9).

Determination of the weight and water and fat contents of the of *B. tabaci* nymphs

The lowest changes in weight were observed at 24-36 h. At 72 h, the weight of the infected group was 0.78-fold that of the control (Fig. 10).

The water content of *B. tabaci* continuously decreased after infection with *L. lecanii*. At 72 h, the water contents of the infected and control groups were lowest reaching 56% and 66%, respectively (Fig. 11).

Until 36 h after infection, the changes in fat content were not significantly different from the control level. At 72 h, the fat content of the infected and control groups was the lowest, reaching 13% and 20.5%, respectively (Fig. 12).

Discussion

The fungus penetrated the insect epidermis via the germ tubes and appressoria, following which the conidia invaded the nymphs and began to enter the haemocoel. Ultimately, the hyphae covered the host surface and had colonized the body cavity (Zhou et al., 2017). Previously, *L. lecanii* caused over 90% mortality of vegetable pest, such as aphids, *Plutella xylostella* (Keppanan et al., 2018; Saruhan, 2018; Sugimoto et al., 2003). In this study, mortality increased greatly during the first 5 d of infection, with the maximum mortality is 82.22% being reached on the 6th day. Accordingly, the activities of detoxification and protective enzymes were lowest on the 5th day, indicating that as the infected nymphs of *B. tabaci* neared death on the 5th day, their

enzyme activity was reduced.

Insects are protected from the stresses of adverse conditions by various physical barriers, including a cuticular exoskeleton, peritrophic membrane, and an immune system that reduces pathogen infection (Chen and Lu, 2017). These fungi stimulate the stress responses of the insect detoxification system and the protective enzyme system under adverse conditions by changing the function of ion channels (Zhang et al., 2017). The major components of the antioxidant defense system of insects include the antioxidant enzymes SOD, CAT, and POD (Li et al., 2016b). When insects are stimulated by exogenous compounds, SOD converts the superoxide radical O_2 into H_2O_2. Then, POD and CAT convert the H_2O_2 into H_2O. The imbalance between oxidative stress and antioxidant responses contributes to disease and the death of insect hosts (Felton and Summers, 1995).

Our study showed that, after infection of *B. tabaci* by *L. lecanii*, the activities of SOD, CAT, and POD initially increased but then decreased thereafter, and the maximum activities protective enzymes were observed on the 2nd day or 3rd day. Previous studies (Yang et al., 2015; Ye et al., 2018; Zhou et al., 2017) indicated agricultural insects infested by entomogenous fungus, the activities of SOD, CAT, and POD initially increased but then decreased. The increased activity of SOD, CAT, and POD effectively preventing the formation of more toxic substances such as hydroxyl radicals and helped increase the resistance of *B. tabaci* (Ding et al., 2015). Under *L. lecanii* infection, ROS and other toxic substances stimulated an immune system response in *B. tabaci* (Li et al., 2016a). To resist the adverse environmental influence and maintain normal physiological activities, the enzyme activities sharply increased. However, the internal spread of the pathogen led to the destruction of the internal tissue structure of the insect and subsequent collapse of the immune system. In addition, the ROS scavenging system might not have been able to remove the excessive quantity of free radicals, leading to reduced enzyme activity and the death of the insect (Li et al., 2016a). So, the activities of SOD, CAT, and POD were decreased on the 5th day. GSTs participate in detoxification metabolism and and catalyze a combination of toxic substances with glutathione and also promote the excretion of toxic chemicals and pathogenic substances (Mathews et al., 2002; Schama et al., 2016). CarEs can catalyze the hydrolysis of ester bonds, and their major physiological functions include lipid metabolism, detoxification metabolism of exogenous compounds and biochemical regulatory functions (Guo et al., 2015). AchE is a target for organophosphorus and carbamate insecticides (Ding et al., 2001). Some exogenous compounds, such as pesticides and pathogenic fungi, can be altered by insect detoxification enzymes. This suggests that *L. lecanii* can promote the detoxification metabolism of *B. tabaci*, which is beneficial for the discharge of exogenous toxicants. With the increase in the level of *B. tabaci* infection with *L. lecanii* exposure time, the exogenous toxicants

overpowered the detoxification metabolism, resulting in the eventual reduction in enzyme activities, and ultimately, insect death. We found that the activities of CarEs, AchE, and GST initially increased but then decreased, and the maximum activities of CarEs, AchE, and GST were observed on the 2nd day or 3rd day after infection. Effects of *Isaria fumosorosea* infection on different enzyme activities in the adult in vivo of *Bemisia tabaci* indicated that the maximum activities of GSTs and CarE were observed on the 48-60h (Tian et al., 2016a). Besides, these findings are similar to previous study (Liu et al., 2013; Zhang et al., 2015). Insects infested with entomopathogenic fungi initially exhibit elevated enzyme activities that decline as the fungal infection continues (Tian et al., 2016a). The entomopathogenic fungus *L. lecanii* can be used to control *B. tabaci* nymphs, but the prevention and control effect is slower than with chemical insecticides. However, the use of entomopathogenic fungi in combination with insecticides to control pests could increase their speed and efficacy (Purwar and Sachan, 2006).

A study of the pathogenicity and control potential of *Beauveria bassiana* on the onion fly showed that the weight increment was smallest after 48 h. The water content and fat content continued to decrease, and the water content and fat content of the infection level were 0.81-fold and 0.69-fold that of the control level, respectively, at 72 h (Zhang, 2017). Screening of the strains of the highly pathogenic *B. bassiana* on soybean pod borers and the assessment biophysical and biochemical effects on their hosts indicated reductions in weight, water content, and fat content (Tian, 2014). These studies corroborate our findings. In the present study, *B. tabaci* nymphs infested with *L. lecanii* JMC-01 gradually lost vitality until death. This process causes many physiological changes in the insects. Thus, *L. lecanii* could constitute a useful alternative biopesticide for *B. tabaci* population management. Biocontrol can reduce insecticide resistance and increase environmental and non-target organism safety.

Conclusions

We observed that *L. lecanii* JMC-01 affected the viability of the *B. tabaci* Q-biotype, by inducing mortality, affecting the activities of protective and detoxifying enzymes, and by significantly reducing the weight, and water and fat content. Thus, *L. lecanii* impacted the physiological functioning of *B. tabaci* by directly acting on molecular targets and by indirectly acting on detoxification and protective enzymes (Bantz et al., 2018). These results indicate that this fungal strain could constitute an effective biological control for *B. tabaci* in agriculture.

Acknowledgments

We thank the private greenhouse owner for access to their greenhouse. We are grateful to Master Kai Gao for providing the biotype of *B. tabaci* and we to Master Hui Wang for helping with the formatting of this paper. We are grateful to two anonymous reviewers and Jasmine Janes for their comments on an early version of the manuscript. We thank LetPub (www.letpub.com) for its linguistic assistance during the preparation of this manuscript.

References

Askary, H, N Benhamou and J. Brodeur 1999. Ultrastructural and Cytochemical Characterization of Aphid Invasion by the Hyphomycete *Verticillium lecanii*. Journal of Invertebrate Pathology 74: 1-13.

Bantz, A, J Camon, J.A Froger, D Goven and V. Raymond 2018. Exposure to sublethal doses of insecticide and their effects on insects at cellular and physiological levels. Current Opinion in Insect Science 30: 73-78. doi: 10.1016/j.cois.2018.09.008.

Barro, P. J. De 2011. Bemisia tabaci, the Capacity to Invade.

Chen, K.K and Z.Q. Lu 2017. Immune responses to bacterial and fungal infections in the silkworm, *Bombyx mori*. Developmental Comparative Immunology 83: 3-11. doi: 10.1016/j.dci.2017.12.024.

Ding, J. N., H. H. Zhang and Defu Chi 2015. Effects of a Pathogenic Beauveria bassiana (Hypocreales: Cordycipitaceae) Strain on Detoxifying and Protective Enzyme Activities in Xylotrechus rusticus (Coleoptera: Cerambycidae) larvae.

Ding, S.Y, H.Y Li, X.F Li and Z.Y Zhang 2001. Effects of Bt Transgenic Poplar on Detoxification Enzyme and AChE in American White Moth Larvae. Journal of Northeast Forestry University 29: 28-29. doi: 10.13759/j.cnkI.dlxb.2001.03.007.

Duan, Y.L, H Wu, Z.Y Ma, L Yang and D.Y. Ma 2017. Scanning electron microscopy and histopathological observations of *Beauveria bassiana* infection of Colorado potato beetle larvae. Microbial Pathogenesis 111. doi: 10.1016/j.micpath.2017.09.025.

Esmail, S.M, R.O Omara, K.A.A Abdelaal and Y.M. Hafez 2018. Histological and biochemical aspects of compatible and incompatible wheat-*Puccinia striiformis* interactions.

Felton, G.W and C.B. Summers 1995. Antioxidant systems in insects. Archives of Insect Biochemistry Physiology 29:

187-197.

Foyer, C. H and G. Noctor 2013. Redox Signaling in Plants. Antioxid Redox Signal 18: 2087-2090. doi: 10.1089/ars.2013.5278

Gao, K. 2018. Biotype Identification and Control of *Bemisia tabaci* in Ningxia. ningxia University.

Ghaffari, S, J Karimi, S Kamali and E.M. Moghadam 2017. Biocontrol of *Planococcus citri* (Hemiptera: Pseudococcidae) by *Lecanicillium longisporum* and *Lecanicillium lecanii* under laboratory and greenhouse conditions. Journal of Asia-Pacific Entomology 20: 605-612. doi: 10.1016/j.aspen.2017.03.019.

Guo, L.T, W Xie, S.L Wang, Q.J Wu, R.M Li, N Yang, X Yang, H.P Pan and Y.J. Zhang 2015. Detoxification enzymes of *Bemisia tabaci* B and Q: biochemical characteristics and gene expression profiles. Pest Management Science 70: 1588-1594. doi: 10.1002/ps.3751

Jiang, L. 2018. Biological Characterizatics of *Lecanicillium lecanii* and Synergistic with Insecticides *Bemisia tabaci*. ningxia University.

Keppanan, R, S Sivaperumal, H Mubasher, C.K Dash, B.S Bamisope, Q Muhammad and L.D Wang 2018. Investigation and molecular docking studies of Bassianolide from *Lecanicillium lecanii* against *Plutella xylostella* (Lepidoptera: Plutellidae).

Lacey, L. A., R Frutos, H. K. Kaya and P. Vail 2001. Insect pathogens as biological control agents: Do they have a future?[Review]. Biological Control 21: 230-248. doi: 10.1006/bcon.2001.0938.

Li, S.G, T.T Dou, X.L Fu, Z.Q Liu and H. Chao 2016a. Changes of protective enzyme activities in *Pieris rapae* infected by *Metarhizium anisopliae*. Plant Protection 42: 133-136. doi: 10.3969/j.issn.0529-1542.2016.03.022.

Li, X.Y, Q.Z Liu, E.E Lewis and E. Tarasco 2016b. Activity changes of antioxidant and detoxifying enzymes in *Tenebrio molitor* (Coleoptera: Tenebrionidae) larvae infected by the entomopathogenic nematode *Heterorhabditis beicherriana* (Rhabditida: Heterorhabditidae). Parasitology Research 115: 1-10. doi: 10.1007/s00436-016-5235-7.

Liu, S.A, Y.G Fu, W.R Huang, B.L Fu and D.Q. Zeng 2013. Variation in the activities of protective and detoxification enzymes in *Aleurodicus dispersus* infected by *Verticillium lecanii*. Plant Protection 39: 7-11. doi: 10.3969/j.issn.0529-1542.2013.03.002.

Liu, W.M, Y.P Xie, J.L Xue, Y Gao, Y.F Zhang, X.M Zhang and J.S Tan 2009. Histopathological changes of *Ceroplastes japonicus* infected by *Lecanicillium lecanii*. Journal of Invertebrate Pathology 101: 96-105. doi: 10.1016/j.jip.2009.03.002.

Mathews, P.M, C.B Guerra, Y Jiang, O.M Grbovic, B.H Kao, S.D Schmidt, R Dinakar, M Mercken, A Hillerehfeld, J

Rohrer, P Mehta, A.M Cataldo and R.A. Nixon 2002. Alzheimer's Disease-related Overexpression of the Cation-dependent Mannose 6-Phosphate Receptor Increases Aβ Secretion. Journal of Biological Chemistry 277: 5299-5307.

Purwar, J.P and G.C. Sachan 2006. Synergistic effect of entomogenous fungi on some insecticides against Bihar hairy caterpillar *Spilarctia obliqua* (Lepidoptera: Arctiidae). Microbiological Research 161: 38-42. doi: 10.1016/j.micres.2005.04.006.

Saruhan, I. 2018. Efficacy of some entomopathogenic fungi against *Aphis fabae Scopoli* (Hemiptera: Aphididae). Egyptian Journal of Biological Pest Control. doi: 10.1186/s41938-018-0096-2.

Schama, R, N Pedrini, M. P Juarez, D. R Nelson, A. Q Torres, D Valle and R. D. Mesquita 2016. *Rhodnius prolixus* supergene families of enzymes potentially associated with insecticide resistance. Insect Biochemistry Molecular Biology 69: 91-104. doi: 10.1016/j.ibmb.2015.06.005.

Shinya, R, D Aiuchi, A Kushida, M Tani, K Kuramochi and M. Koike 2008. Effects of fungal culture filtrates of *Verticillium lecanii* (*Lecanicillium* spp.) hybrid strains on *Heterodera glycines* eggs and juveniles. Journal of Invertebrate Pathology 97: 291-297. doi: 10.1016/j.jip.2007.11.005.

Sugimoto, M, M Koike, N Hiyama and H. Nagao 2003. Genetic, morphological, and virulence characterization of the entomopathogenic fungus *Verticillium lecanii*. Journal of Invertebrate Pathology 82: 176-187. doi: 10.1016/S0022-2011(03)00014-4.

Tang, X.T, L Cai, Y Shen and Y.Z. Du 2018. Diversity and evolution of the endosymbionts of *Bemisia tabaci* in China. PeerJ. doi: 10.7717/peerj.5516.

Tian, J, H.L Diao and R.Y. Ma 2016a. Effects of *Isaria fumosorosea* Infection on Different Enzyme Activities in the Adult in vivo of *Bemisia tabaci*. Journal of Shanxi Agricultural Sciences 44: 1007-1010. doi: 10.3969/j.issn.1002-2481.2016.07.27.

Tian, S, X.B Wang, P Li, H Wang, H.T Ji, J.Y Xie, Q.L Qiu, D Shen and H.S Dong 2016b. Plant Aquaporin AtPIP1;4 Links Apoplastic H_2O_2 Induction to Disease Immunity Pathways. Plant Physiology 171: 1635-1650. doi: 10.1104//pp.15.01237

Tian, Y.Z. 2014. The Screening of the Strains of the High Pathological *Beauveria bassiana* on Soybean pod borers and the Biophysical and Biochemical Effects on Their Hosts. Jilin Agricultural University.

Wang, Z.L, Z Zhao, X.F Cheng, S.Q Liu, Q Wei and I.M. Scott 2016. Conifer flavonoid compounds inhibit detoxification enzymes and synergize insecticides. Pesticide Biochemistry and physiology 127: 1-7. doi: 10.1016/j.pestbp.2015.09.003.

Xie, M, J.Y Zhang, D.L Peng, J Zhou, X.L Zhang, Z.R Zhang, J.J Zhao and Y.H. Wu 2015. Persistence and Viability of *Lecanicillium lecanii* in Chinese Agricultural Soil. PLOS ONE. doi: 10.1371/journal.pone.0138337.

Xu, Q.Y, F.H Chai, X.C An and S.C Han 2014. Comparison of Detoxification Enzymes of *Bemisia tabaci* (Hemiptera: Aleyrodidae) Biotypes B and Q After Various Host Shifts. Florida Entomologist 97: 715-723. doi: 10.1653/024.079.0253.

Xu, Y.L, Z.Y Wang, K.L He and S.Xiong. Bai 2006. Effects of transgenic Bt corn expressing Cry1Ab toxin on activities of some enzymes in larvae of the Asian corn borer, *Ostrinia furnacalis* (Guenée) (Lepidoptera: Pyralidae). Acta Entomologica Sinica 49: 562-567. doi: 10. 16380/ j. kcxb. 2006. 04. 005.

Yang, Q, S.H Wang, W.H Zhang, T.T Yang and Y.J. Liu 2015. Toxicity of commonly used insecticides and their influences on protective enzyme activity of multicolored Asian lady beetle *Harmonia axyridis*(Pallas). Journal of Plant Protection 42: 258-263. doi: 10.13802/j.cnki.zwbhxb.2015.02.017.

Ye, B.H, Y.B Zhang, J.P Shu, H Wu and X.J. Wang 2018. Effects of Three Different *Metarhizium* Strains on Virulence and Protective Enzymes Activities of *Melanotus cribricollis* larvae. Scientia Silvae Sinicae 54: 100-108. doi: 10.11707/j.1001-7488.20180612.

Zare, R and W. Gams 2001. A revision of *Verticillium* sect. Prostrata. VI. The genus *Haptocillium*. Nova Hedwigia 73: 1-50.

Zhang, H, S.Y Wu, S.Y Wang and Z.R. Lei 2017. Effect of *Beauveria bassiana* on the Activity of Defense Enzymes and Cellular Defense Response of Adult of *Delia antiqua*(Meigen). Chinese Journal of Biological Control 33: 198-205. doi: 10.16409/j.cnki.2095-039x.2017.02.009.

Zhang, H. 2017. Research on Virulence and Control Effect of *Beauveria bassiana* against Onion Maggot (Diptera: Anthomyiidae) Chinese Academy of Agricultural Sciences Dissertation.

Zhang, Y.F, Z.H Wang, X.Q Nong, G.C Cao, Z Li, G.J Wang and Z.H Zhang 2015. Effect of *Metarhizium anisopliae* on Protective Enzyme and Detoxification Enzyme in the Midgut of *Locusta migratoria manilensis*. Chinese Journal of Biological Control 31: 876-881. doi: 10.16409/j. cnki. 2095-039x. 2015. 06. 009.

Zhou, J.Y, M.K Liu, L.N Xiao, D.X Chen, C.Y Ren, C.Q Diao, G.C Zhang, X.Q Wang and M.Y. Li 2017. Screening of high virulent isolate of *Beauveria* spp. against *Helicoverpa assulta* and changes of protective enzymes activities in the larvae infected by fungi. Journal of Anhui Agricultural University 44: 1119-1123. doi: 10.13610/j.cnki.1672-352x.20171214.034.

Zhu, H and J.J Kim 2011. Susceptibility of the tobacco whitefly, *Bemisia tabaci* (Hemiptera: Aleyrodidae) biotype Q to entomopathogenic fungi. Biocontrol Science Technology 21: 1471-1483. doi: 10.1080/ 09583157.2011.636482.

513

Figure 1

Morphological characteristics of the *B. tabaci* nymph induced by *L. lecanii* JMC-01

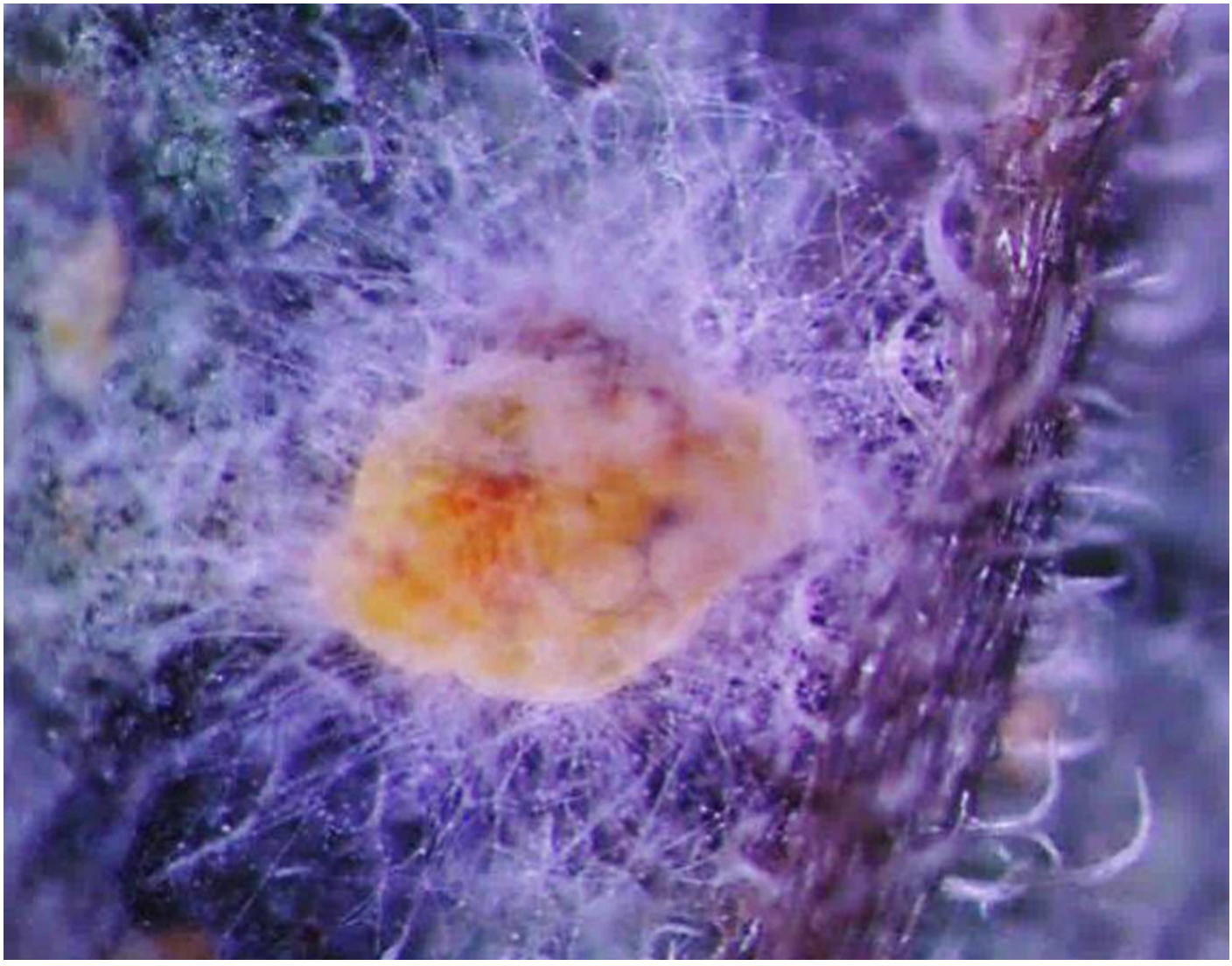

Figure 2

Cumulative corrected mortality of *L. lecanii* JMC-01 infestation on *B. tabaci* nymphs

Note: times marked with different uppercase letters on the same line are significantly different (P<0.05). The different lowercase letters indicate significant differences between the treatment and control groups (P<0.05) at the same time point.

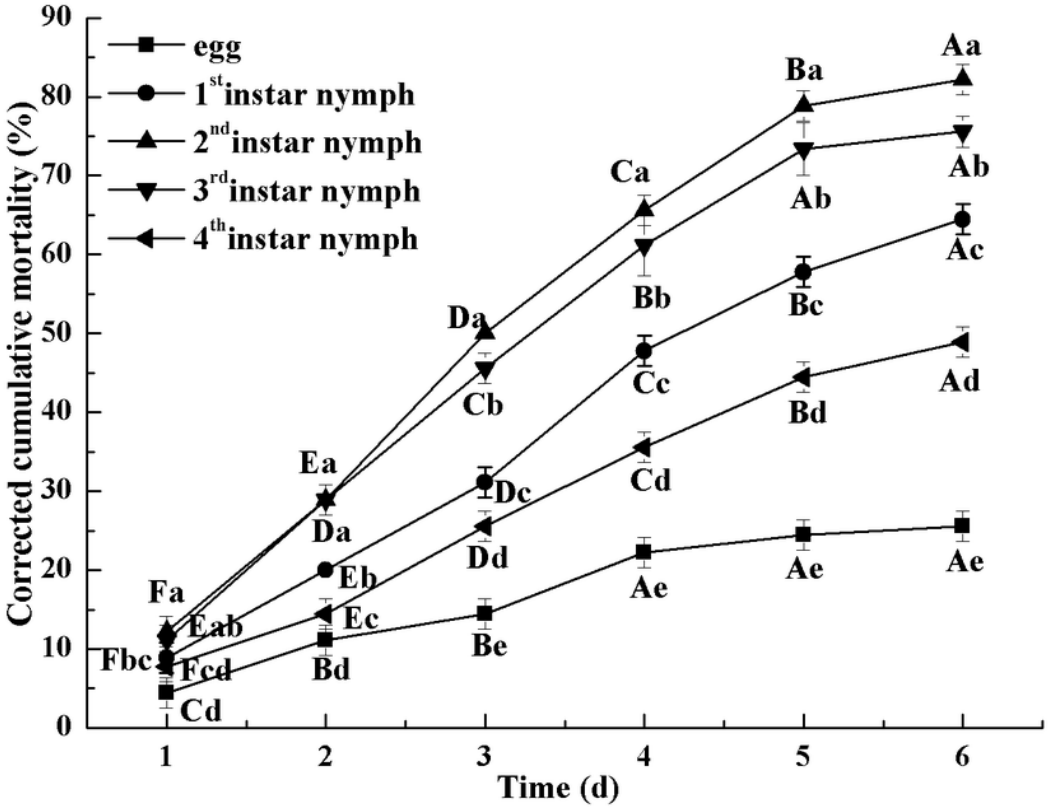

Figure 3

Cumulative corrected mortality of the 3rd-instar *B. tabaci* nymphs following exposure to different concentrations of *L. lecanii* JMC-01

Each data point indicates the corrected cumulative mortality for each time period

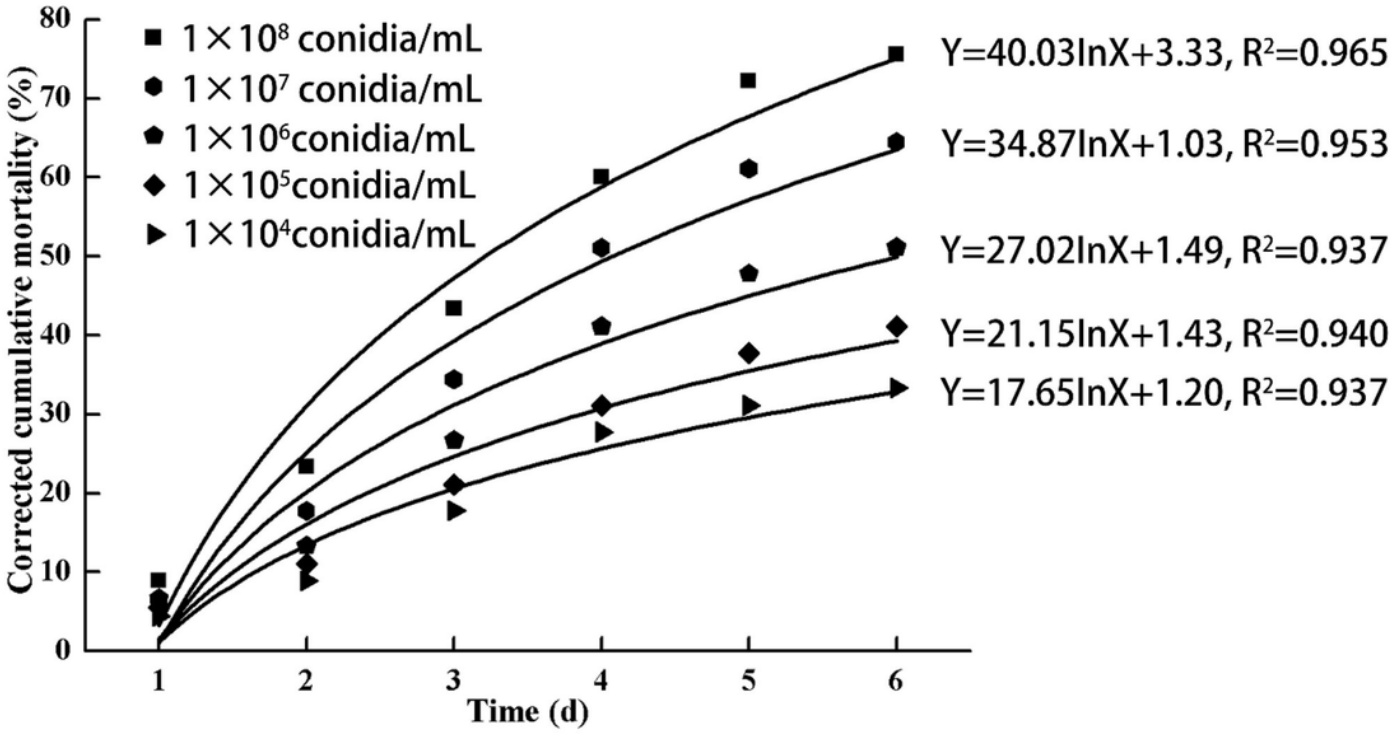

Figure 4

Effects of SOD activities of the 3rd-instar *B. tabaci* nymphs infested with *L. lecanii* JMC-01

Note: times marked with different uppercase letters on the same line are significantly different (P<0.05). The different lowercase letters indicate significant differences between the treatment and control groups (P<0.05) at the same time point.

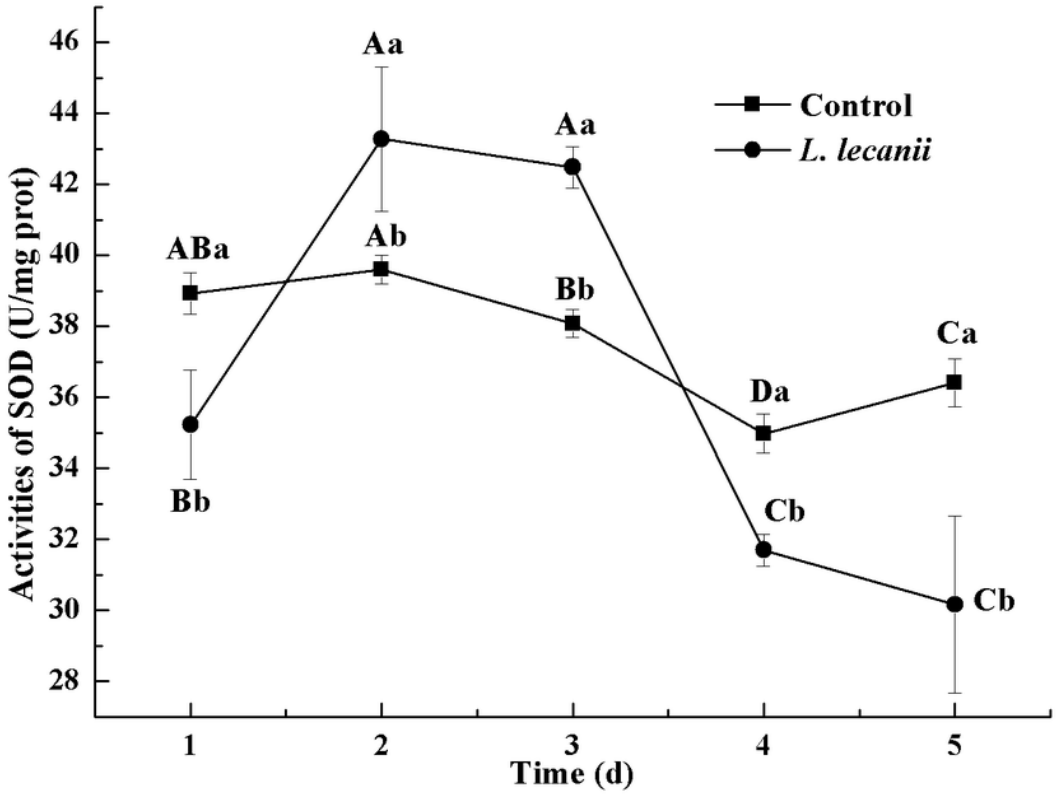

Figure 5

Effects of POD activities of the 3rd-instar *B. tabaci* nymphs infested with *L. lecanii* JMC-01

Note: times marked with different uppercase letters on the same line are significantly different (P<0.05). The different lowercase letters indicate significant differences between the treatment and control groups (P<0.05) at the same time point.

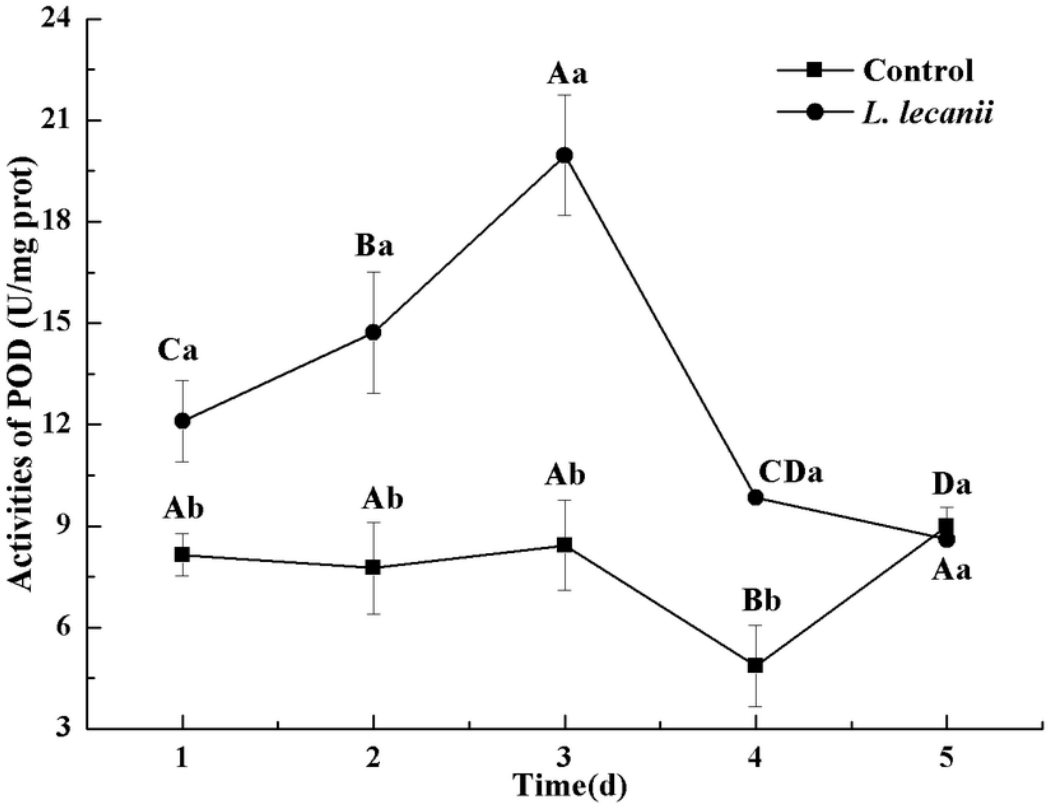

Figure 6

Effects of CAT activities of the 3rd-instar *B. tabaci* nymphs infested with *L. lecanii* JMC-01

Note: times marked with different uppercase letters on the same line are significantly different (P<0.05). The different lowercase letters indicate significant differences between the treatment and control groups (P<0.05) at the same time point.

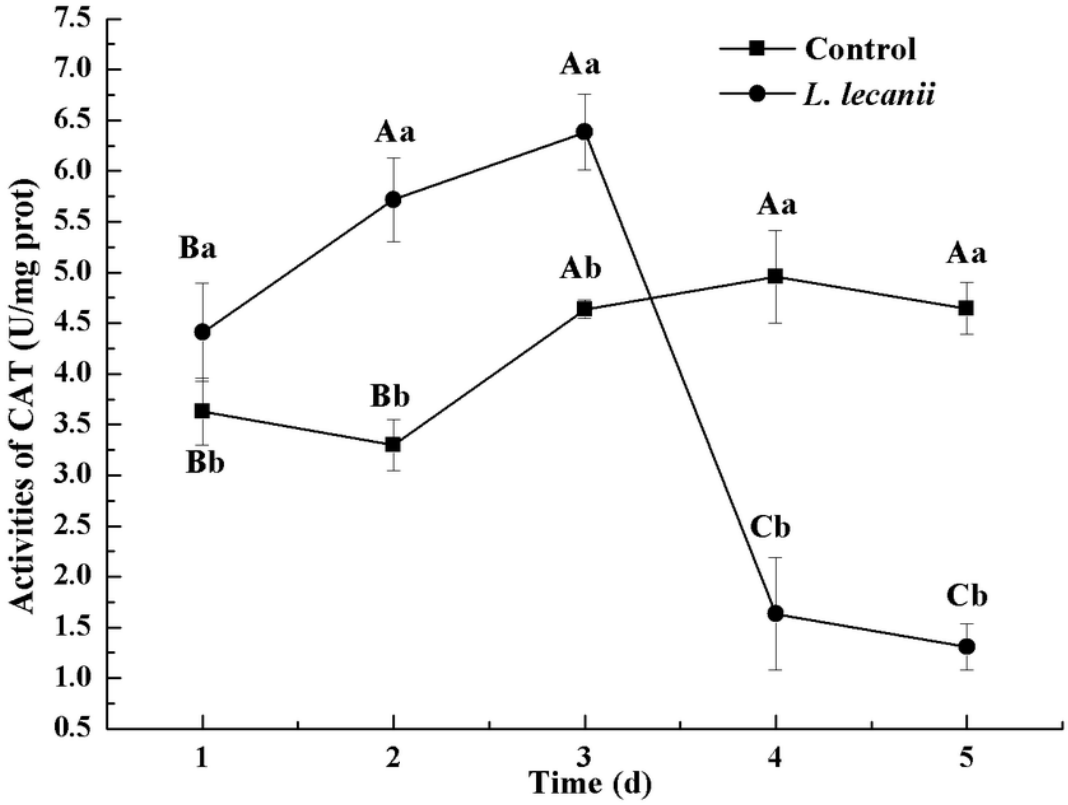

Figure 7

Effects of CarE activities of the 3rd instar nymph of *B. tabaci* infested with *L. lecanii* JMC-01

Note: times marked with different uppercase letters on the same line are significantly different (P<0.05). The different lowercase letters indicate significant differences between the treatment and control groups (P<0.05) at the same time point.

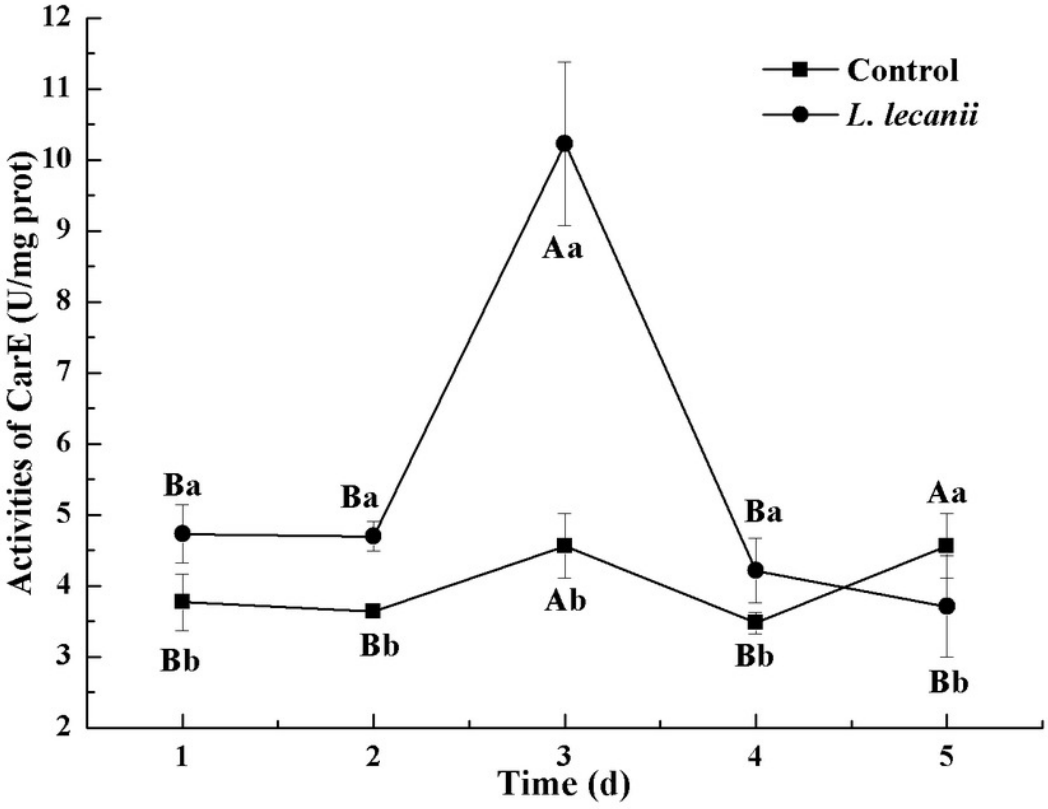

Figure 8

Effects of AchE activities of the 3rd instar nymph of *B. tabaci* infested with *L. lecanii* JMC-01

Note: times marked with different uppercase letters on the same line are significantly different (P<0.05). The different lowercase letters indicate significant differences between the treatment and control groups (P<0.05) at the same time point.

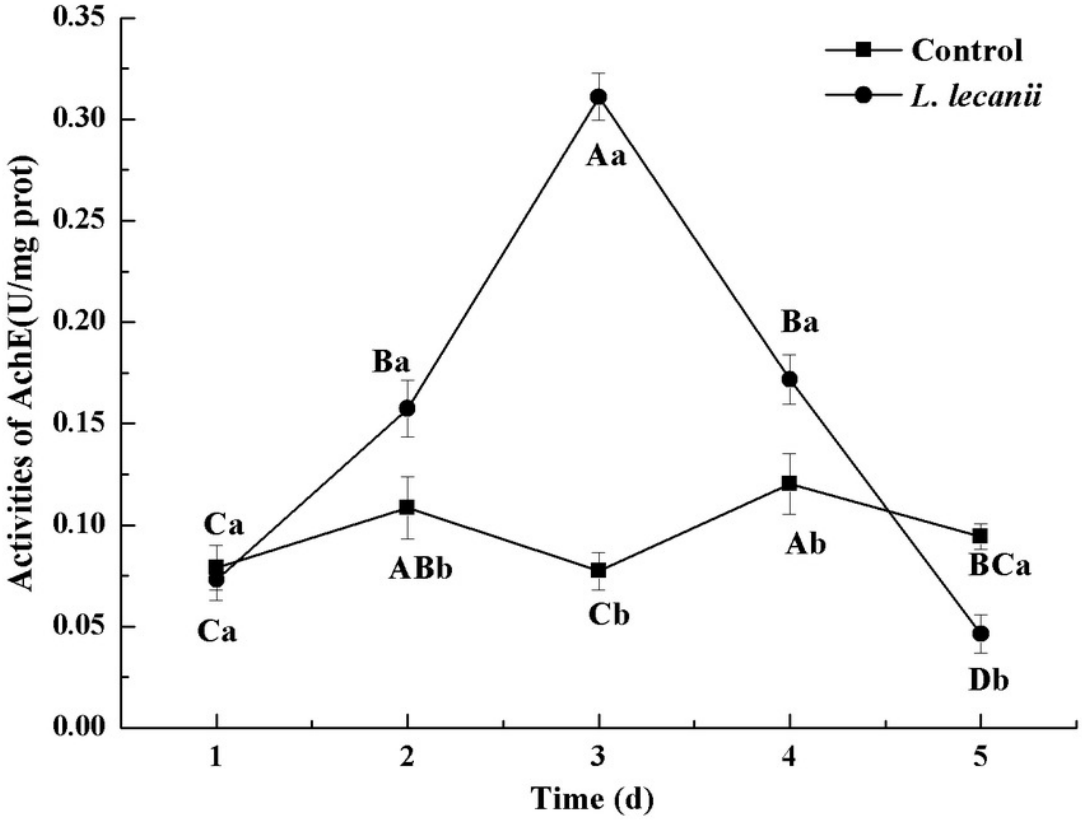

Figure 9

Effects of GST activities of the 3rd instar nymph of *B. tabaci* infested with *L. lecanii* JMC-01

Note: times marked with different uppercase letters on the same line are significantly different (P<0.05). The different lowercase letters indicate significant differences between the treatment and control groups (P<0.05) at the same time point.

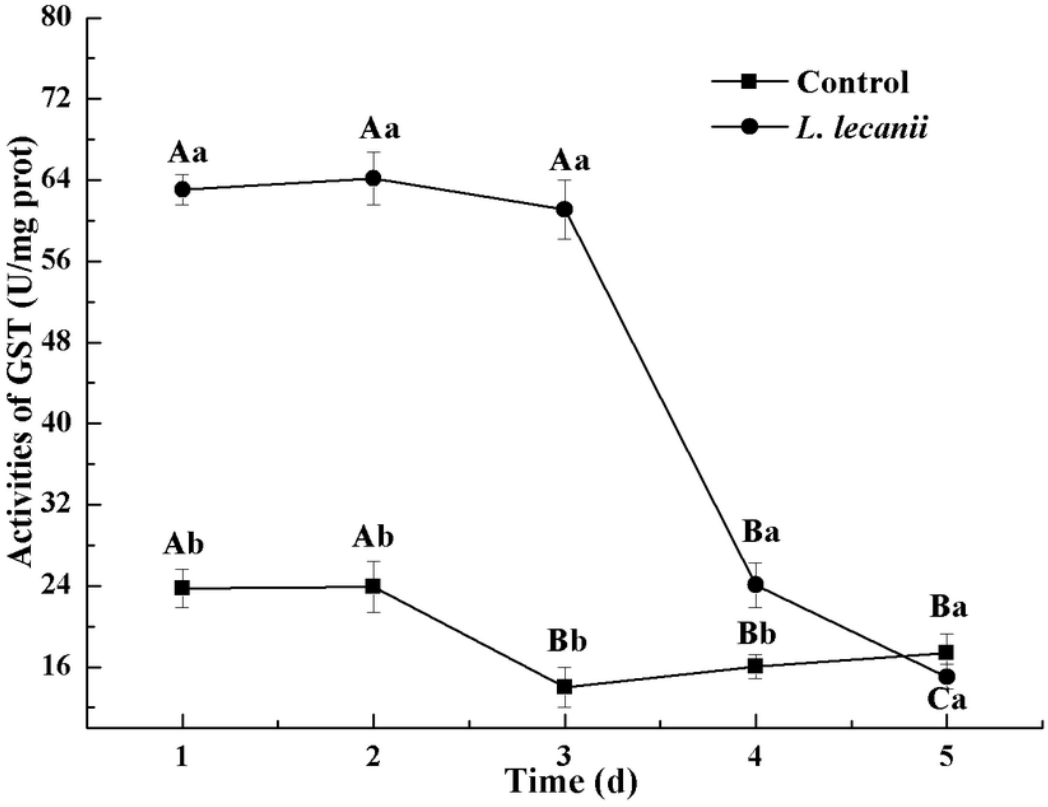

Figure 10

Changes in weight of the 3rd instar *B. tabaci* nymphs infected with *L. lecanii* JMC-01

Note: times marked with different uppercase letters on the same line are significantly different (P<0.05). The different lowercase letters indicate significant differences between the treatment and control groups (P<0.05) at the same time point.

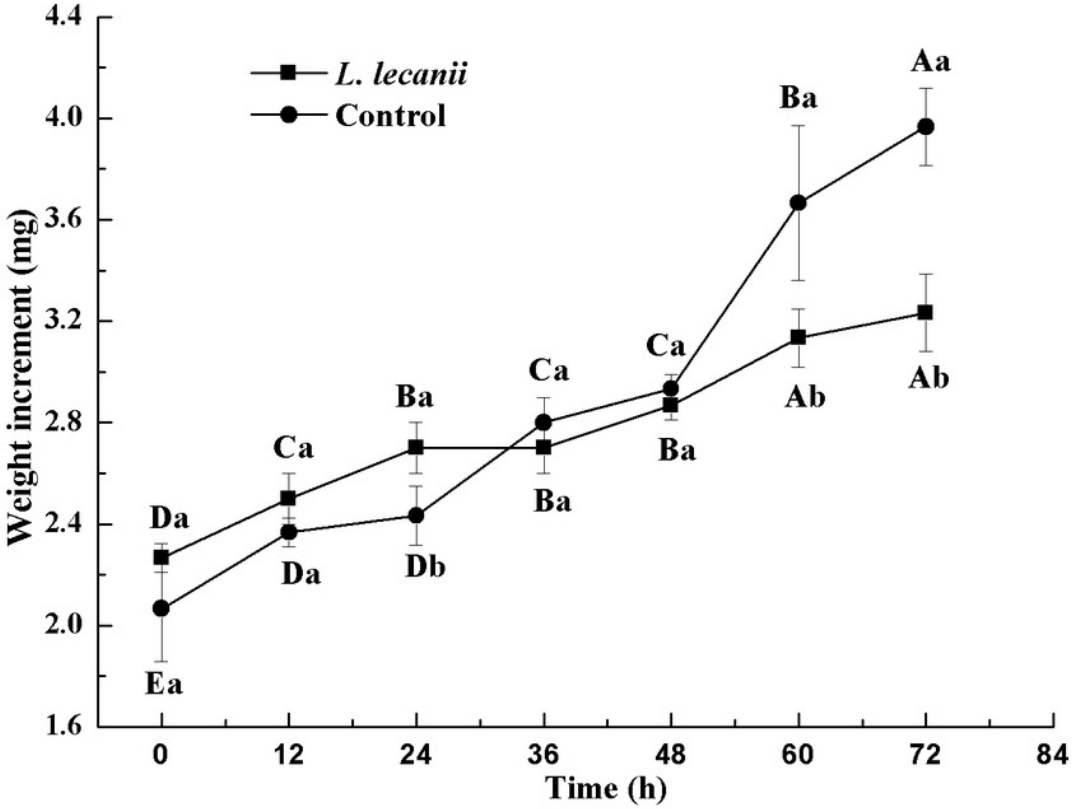

Figure 11

Changes in water content of the 3rd instar *B. tabaci* nymphs infected with *L. lecanii* JMC-01

Note: times marked with different uppercase letters on the same line are significantly different (P<0.05). The different lowercase letters indicate significant differences between the treatment and control groups (P<0.05) at the same time point.

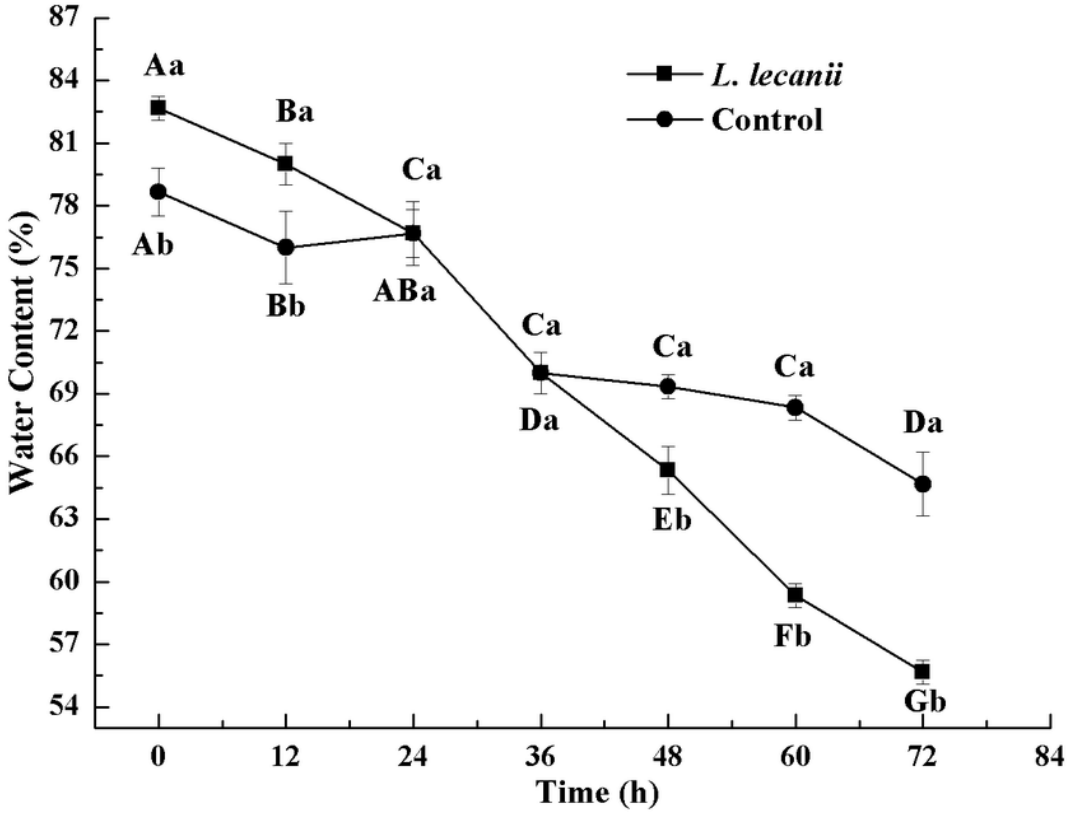

Figure 12

Changes in and fat content of the 3rd instar *B. tabaci* nymphs infected with *L. lecanii* JMC-01

Note: times marked with different uppercase letters on the same line are significantly different (P<0.05). The different lowercase letters indicate significant differences between the treatment and control groups (P<0.05) at the same time point.

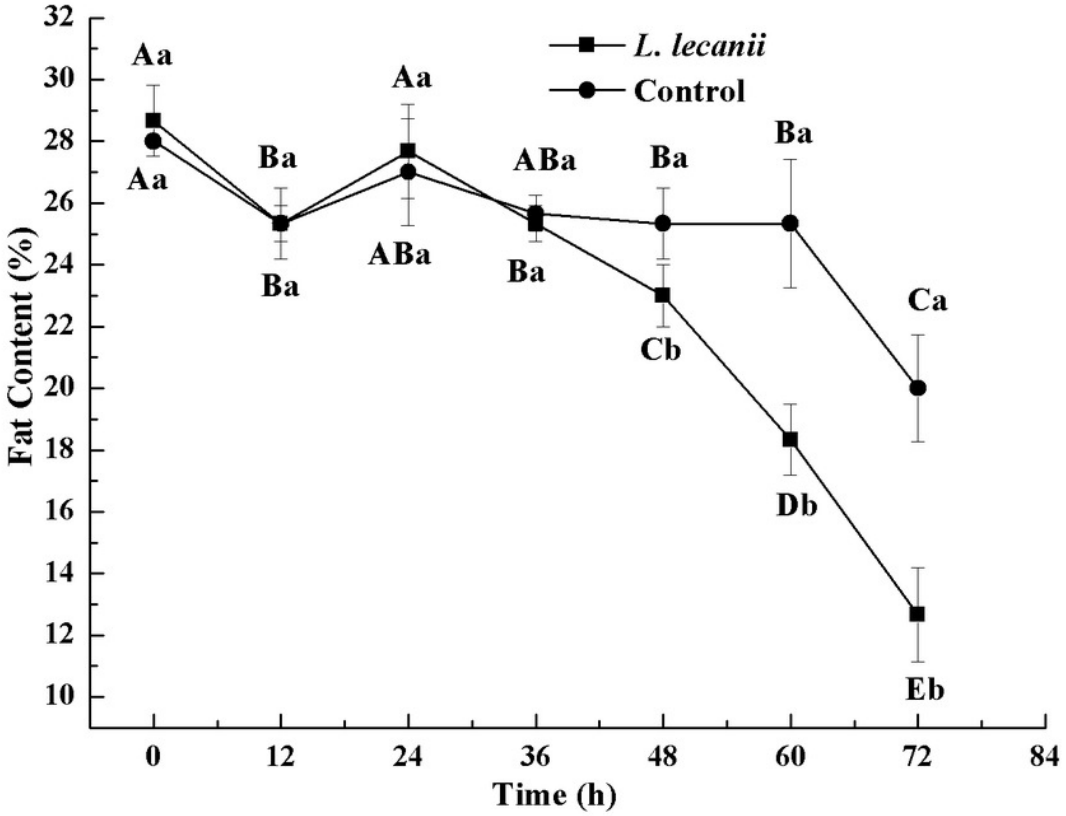

Table 1(on next page)

The steps of protein content determination are described in the table 1

1 Table 1

	Blank tube	Standard tube	Measuring tube
Double distilled water (μL)	20		
563μg/ml standard solution (μL)		20	
Sample (μL)			20
Working fluid (μL)	250	250	250
Mix, set at 37 °C water bath for 30 min (digital thermostat water bath)			
Stop application solution (μL)	750	750	750

2

Table 2(on next page)

The steps of SOD activity determination are described in the table 2

1 Table 2

Reagent	Measuring tube	Control tube
Reagent one application solution (mL)	1.0	1.0
Sample (mL)	0.1	
Double distilled water (mL)		0.1
Reagent two solution (mL)	0.1	0.1
Reagent three solution (mL)	0.1	0.1
Reagent four application solution (mL)	0.1	0.1
Mix, set at 37 °C water bath for 40 min (digital thermostat water bath)		
Chromogen solution (mL)	2	2

2

Table 3(on next page)

The steps of POD activity determination are described in the table 3

1 Table 3

	Blank tube	Measuring tube
Reagent one solution (mL)	2.4	2.4
Reagent two application solution (mL)	0.3	0.3
Reagent three application solution (mL)	0.2	0.2
Double distilled water (mL)	0.1	
Sample (mL)		0.1
Set at 37 °C water bath for 30 min (digital thermostat water bath)		
Reagent four (mL)	1.0	1.0

2

Table 4(on next page)

The steps of CAT activity determination are described in the table 4

Table 4

	Control tube	Measuring tube
Sample (mL)		0.05
Reagent one solution (37°C preheat) (mL)	1.0	1.0
Reagent two solution (37°C preheat) (mL)	0.1	0.1
Mix, set at 37 °C water bath for 1 min (digital thermostat water bath)		
Reagent three solution (mL)	1.0	1.0
Reagent four solution (mL)	0.1	0.1
Sample (mL)	0.05	

Table 5(on next page)

The steps of AchE activity determination are described in the table 5

The same sample was added to the control tube and the measuring tube, but the order was different. The blank tube was not sampled and distilled water was used instead of the sample.

1 Table 5

	Measuring tube	Control tube	Standard tube	Blank tube
Sample (mL)	0.1			
1μmol/mL standard application solution (mL)			0.1	
Double distilled water (mL)				0.1
Substrate buffer (mL)	0.5	0.5	0.5	0.5
Chromogen application solution (mL)	0.5	0.5	0.5	0.5
Mix, set at 37 °C water bath for 6 min (digital thermostat water bath)				
Inhibitor solution (mL)	0.03	0.03	0.03	0.03
Transparent solution (mL)	0.1	0.1	0.1	0.1
Sample (mL)		0.1		

2

Table 6(on next page)

The steps of enzymatic reaction are described in the table 6

1 Table 6

	Measuring tube	Control tube
Matrix fluid (mL)	0.3	0.3
Sample (mL)	0.1	
Mix, set at 37 °C water bath for 10 min (digital thermostat water bath)		
Reagent two application solution (mL)	1	1
Anhydrous alcohol l(mL)	1	1
Sample (mL)		0.1

2

Table 7 (on next page)

The steps of chromogen reaction are described in the table 7

The same sample was added to the control tube and the measuring tube, but the order was different. The blank tube was not sampled and distilled water was used instead of the sample.

1 Table 7

	Blank tube	Standard tube	Measuring tube	Control tube
GSH strandard application solution (mL)	2			
20μmol/mL GSH strandard solution (mL)		2		
Supernatant (mL)			2	2
Reagent three application solution (mL)	2	2	2	2
Reagent four application solution (mL)	0.5	0.5	0.5	0.5

2